Biofilm Formation on Chromatic Sol–Gel/Polydiacetylene Films

Margarita Ritenberg,[b] Sofiya Kolusheva,[a] Hadas Ganin,[b] Michael M. Meijler,[b] and Raz Jelinek*[a, b]

Bacterial biofilms are integrated, single- or multi-species communities of cells that play profound roles in human health and disease. The formation of biofilms requires interactions between bacteria and the surfaces they colonize, and the surface can specifically impact the structure, function, and composition of these communities. Investigating biofilm formation in situ, their assembly kinetics, and particularly identifying substances that could interfere with or inhibit biofilm growth is thus a major scientific and practical goal. It is shown that thin dip-coated films comprising a transparent sol–gel framework and polydiacetylene, a unique conjugated polymer that can undergo color and fluorescence transitions, both promote rapid growth of bacterial biofilms as well as allow colorimetric and fluorescence detection of biofilm formation. Microscopy data demonstrate that the bacterial cells and resultant biofilm specifically target the polydiacetylene domains embedded within the silica-gel matrix, consequently inducing dramatic colorimetric and fluorescence transitions. The mesoporous silica/polydiacetylene matrix can further host other chemical substances allowing evaluation of their biofilm inhibitory effects through simple chromatic screening. Overall, the polydiacetylene/sol–gel films constitute a novel generic platform for promoting bacterial biofilms and their in situ analysis.

Introduction

Bacterial biofilms are integrated communities of cells consisting of one or more species joined together in an extracellular polymeric matrix, enabling them to efficiently adhere to surfaces.[1] These multicellular constructs are marked by a high degree of chemical communication and are fundamental to the ecology and biology of most bacterial strains. Owing to the impregnable nature of biofilm frameworks, these matrices result in protection of the embedded bacterial cells and thus high resistance against antibacterial agents.[2] Indeed, not only do biofilms adversely affect human health and promote disease progression, they also play important roles in seemingly unrelated fields of energy generation and environmental degradation.[3, 4]

Biofilms exhibit a wide diversity of structures and molecular compositions, depending on the bacterial species and environmental aspects. A central parameter affecting biofilm formation mechanisms and properties is the adsorption and interactions between the bacterial cells and the surfaces they colonize, and both microbe and surface can impact the structure, architecture, function, and composition of these communities. Bacteria in biofilms exhibit a surprisingly sophisticated level of social behavior, both cooperative and competitive, made possible by their cell biology and chemical communication among cells. As such, biofilm formation is governed by hierarchically organized processes shaped by complex physical and chemical interactions.

Identification of biofilm assemblies is usually carried out through ex situ methods, generally utilizing dyes such as crystal violet to stain the bacteria that remain after washing away the non-adherent bacteria.[5] Other approaches of biofilm analysis employ scanning electron microscopy (SEM), confocal fluorescence microscopy,[6] atomic force microscopy (AFM), and polymerized chain reaction (PCR) for detection of biofilm-associated genetic markers.[7] Development of biofilm detection schemes using specific adherent substrates, such as borosilicate tubes[8] or polystyrene surfaces[9] have been demonstrated. Simple, easily implemented in situ biofilm screening methods, however, are rare, mostly as a result of the complexity of biofilm structures and molecular compositions and the difficulties of assessing biofilm architecture using simple analytical tools.[10] This deficiency imposes a significant limitation for investigating the factors affecting biofilm development, and in particular the identification of possible inhibitors through high-throughput screening techniques.

Herein, we describe detection and analysis of biofilm formation through the use of thin films produced through dip-coating techniques employing silicon dioxide (silica) sol–gel and polydiacetylene (PDA). Polydiacetylene is a conjugated ene–yne polymer assembly produced upon ultraviolet irradiation of ordered diacetylene monomers.[11] Since their introduction in the early 1970s, PDA systems, primarily vesicles and thin films,

[a] Dr. S. Kolusheva, Prof. R. Jelinek
Ilse Katz Institute for Nanoscale Science and Technology
Beer Sheva 84105 (Israel)
E-mail: razj@bgu.ac.il

[b] M. Ritenberg, H. Ganin, Prof. M. M. Meijler, Prof. R. Jelinek
Department of Chemistry, Ben-Gurion University of the Negev
Beer Sheva 84105 (Israel)

have attracted significant scientific and technological interest due to their unique chromatic properties.[12–14] Specifically, PDA matrixes were shown to undergo dramatic visible colorimetric and fluorescence transformations induced by diverse biological and chemical molecules and environmental stimuli, thus making PDA a powerful constituent in sensing platforms.[15–18] Our research group has recently shown that PDA can be utilized for bacterial sensing.[19,20] Particularly important, PDA can be coupled to varied scaffolding materials, thus producing sensors exhibiting diverse configurations and properties.[21,22]

We recently demonstrated the formation of chromatic films comprising PDA derivatives and hexagonal silica through self-assembly at the air/water interface.[23] Herein, we show that sol–gel/PDA films assembled through dip-coating constitute a highly effective substance for initiation and growth of bacterial biofilms, and particularly importantly, allow biofilm analysis in situ through monitoring the chromatic properties of the PDA embedded in the films.

Results and Discussion

Figure 1 A presents a schematic depiction for preparation of silica sol–gel/PDA thin films through the dip-coating technique.[24,25] Briefly, the monomeric constituents (both tetraorthosilicate and diacetylene, respectively) were dissolved in an organic solvent; insertion and slow lifting of the hydrophilic substrate (e.g. glass) resulted in condensation of a silica-gel thin film which also encapsulated diacetylene domains. Ultraviolet irradiation (at 254 nm) of the glass-supported film in-
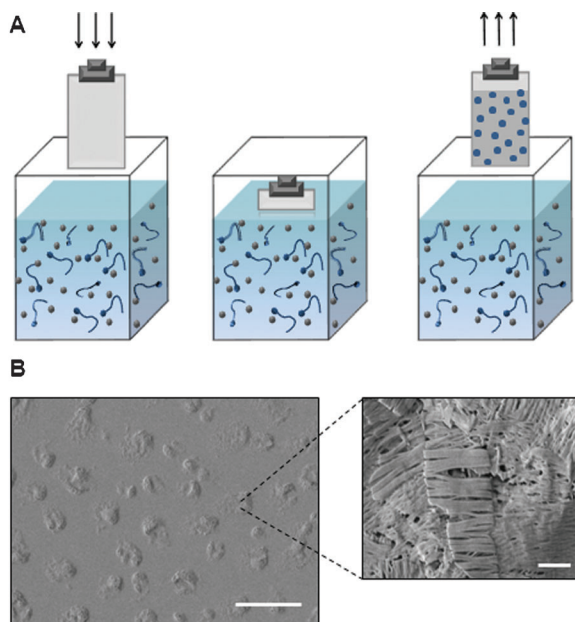

Figure 1. Formation of dip-coated sol–gel/polydiacetylene films. A) schematic showing silica sol-gel/PDA preparation. Gray balls represent the silica monomers, while the blue tailed-balls represent the diacetylene monomer. The dark blue domains on the right drawing correspond to the gel-embedded diacetylene domains. B) SEM image of the sol–gel/PDA surface; the insert highlights the PDA domains comprising the oriented polymer. Scale bars correspond to 50 μm (left) and 0.5 μm (insert on the right).

duced polymerization of the diacetylene units, giving rise to blue PDA. Figure 1 B shows scanning electron microscopy (SEM) images highlighting the film morphology. Specifically, the SEM image in Figure 1 B indicates that abundant PDA domains displaying the typical lamellar-oriented polymeric structures[26,27] were distributed within the sol–gel matrix, protruding at the gel surface.

The dip-coated sol–gel/PDA films were employed in this study as a platform for initiation and analysis of bacterial biofilms and substances involved in biofilm inhibition (Figure 2–Figure 5). Figure 2 A depicts the color properties of the sol–gel/PDA films following incubation with bacterial solutions. Specifi-
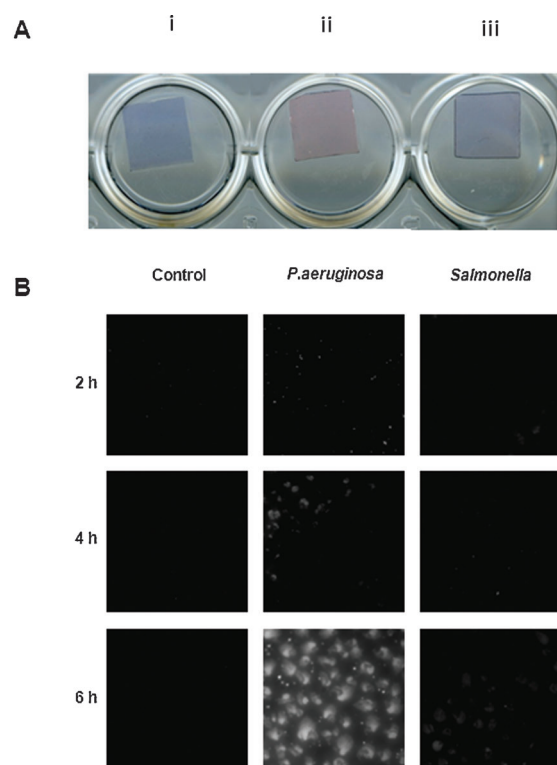

Figure 2. Bacterially induced chromatic transformations in sol–gel/PDA films. A) Images of glass-supported sol–gel/PDA films incubated for 6 hours with *Pseudomonas aeruginosa* (ii), bacterial growth medium (control; i), and Salmonella typhimurium (iii). B) Fluorescence microscopy images (excitation 470 to 490 nm, emission > 520 nm) of sol–gel/PDA films incubated in different bacterial suspensions and recorded at the indicated times. All images correspond to 100 μm×100 μm areas.

cally, Figure 2 A shows the dramatic blue–red transformation occurring following immersion of the sol–gel/PDA film for a few hours in a medium solution containing *Pseudomonas aeruginosa*, an opportunistic pathogen known as a prolific biofilm producer[28] (Figure 2 A ii). Interestingly, incubation of the silica sol–gel/PDA film with a suspension of the bacterium *Salmonella typhimurium,* which does not readily form biofilms, hardly altered the blue color of the film (Figure 2 A iii).

Beside the colorimetric transformations of PDA, one can also exploit the concurrent fluorescence properties of the conjugat-

ed polymer for analysis of bacterially induced chromatic transformations within the sol–gel/PDA matrix. Figure 2B depicts fluorescence microscopy images recorded with a desktop microscope at different times after initiating bacterial growth. Figure 2B shows appearance of fluorescent PDA domains within four hours of co-incubation of the silica sol–gel/PDA films with *P. aeruginosa*, and highly fluorescent PDA patches were apparent six hour after the beginning of incubation with this bacterial species. In contrast to the *Pseudomonas*-induced PDA fluorescence and consistent with the colorimetric data in Figure 2A, significantly less and fainter fluorescent areas were observed when the sol–gel/PDA film was incubated with *Salmonella typhimurium* (Figure 2B). Independent measurements confirmed that both bacterial species prolife-rated in the presence of the sol–gel/PDA films (with *Salmonella* growing even faster than *Pseudomonas*, Figure 1 in the Supporting Information).

Even though Figure 2 establishes a clear correlation between the chromatic transformations of PDA and proliferation of *P. aeruginosa*, further experimental evidence is required to demonstrate that the formation of bacterial biofilms is in fact the cause of color/fluorescence changes. In the experiments presented in Figure 3 we stained both bacterially incubated sol–gel/diacetylene film and sol–gel film (not containing PDA), respectively, with crystal violet—a fluorescent marker commonly employed for staining biofilms and surface-immobilized bacterial cells.[5] Indeed, as the fluorescence microscopy images in Figure 3A–C show, a significant increase in crystal-violet emission following incubation of the films with *P. aeruginosa* indicates that biofilms were indeed deposited over broad surface areas, becoming more abundant in greater incubation times.

Importantly, the crystal violet fluorescence microscopy data and corresponding bright-field images in Figure 3A–C demonstrate that the biofilms appear to specifically develop upon the PDA domains embedded in the silica sol–gel/PDA matrix (note that the PDA domains appear darker than the sol–gel background in the bright field microscopy images). The significance of the PDA domains in promoting biofilm formation is particularly apparent in Figure 3D, which depicts an experiment in which a pure silica-gel dip-coated film was prepared, incubated with *P. aeruginosa*, and subsequently dyed with crystal violet. The fluorescence microscopy image in Figure 3D indicates the occurrence of some adsorption of *P. aeruginosa* bacterial cells onto the film surface, but essentially no biofilm deposition was observed. It should be emphasized that chromatic phenomena similar to Figure 2 and Figure 3 were observed for other biofilm-forming bacterial strains (Figure 3, see the Supporting Information), thus underscoring the generality of the sol–gel/PDA system as a biofilm sensor.

The SEM images in Figure 4 provide dramatic visual evidence for the direct association of the bacterial biofilms with the film-embedded PDA domains. The SEM analysis, carried out using a silica-gel/PDA film incubated for 4 hours in a solution of *P. aeruginosa*, shows that the bacterial cells specifically accumulate upon the PDA domains protruding from the silica-gel surface, and that a biofilm network emerges upon the aggregated bacteria, apparent as the fibrous structures extended
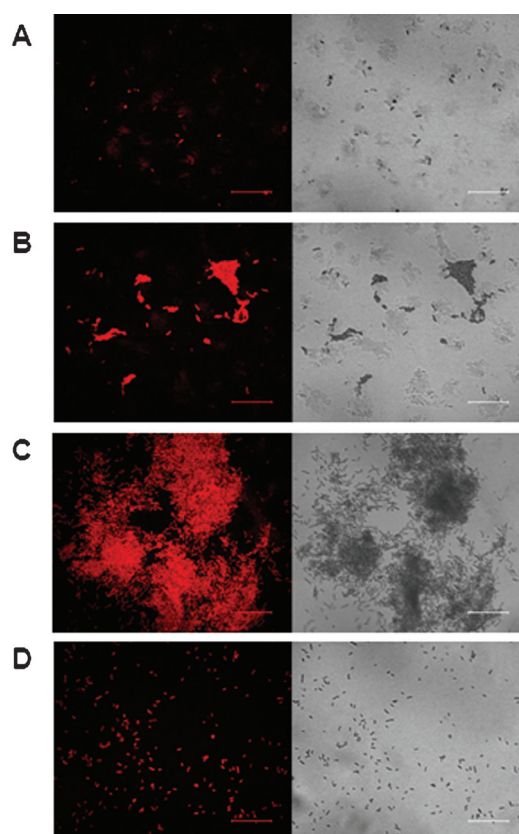

Figure 3. Biofilm formation on sol–gel/PDA films. Left panels: confocal fluorescence microscopy images (excitation 568 nm) of films stained with crystal-violet and incubated with *P. aeruginosa*. Right panels: corresponding bright field images. A) sol–gel/PDA film incubated with *P. aeruginosa* for 2 hours. B) sol–gel/PDA film incubated with *P. aeruginosa* for 6 hours. C) sol–gel/PDA film incubated with *P. aeruginosa* for 8 hours. D) sol–gel film (not containing PDA) incubated with *P. aeruginosa* for 8 hours. Scale bars for all images: 20 µm.
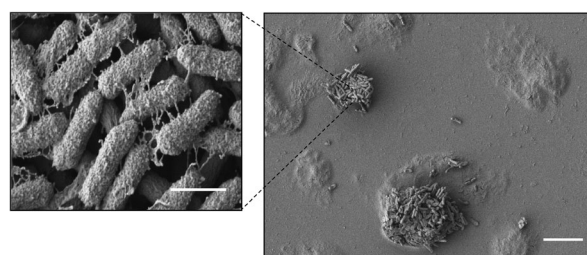

Figure 4. *P. aeruginosa* biofilms formed on the polydiacetylene domains. SEM images showing cell aggregation and biofilm formation upon PDA domains embedded within the sol–gel film matrix. Scale bars: right image 10 µm, left image (inset) 1 µm.

between the cells. Note that the SEM images in Figure 4 indicate that hardly any bacterial cells appear attached to the smooth silica surface. The apparent "capture" of bacterial cells by the PDA domains, resulting in initiation of biofilm formation, might correspond to non-specific cell adhesion to the hydrophobic PDA moieties protruding from the silica gel surface and the rough surface features of the PDA domains.[29]

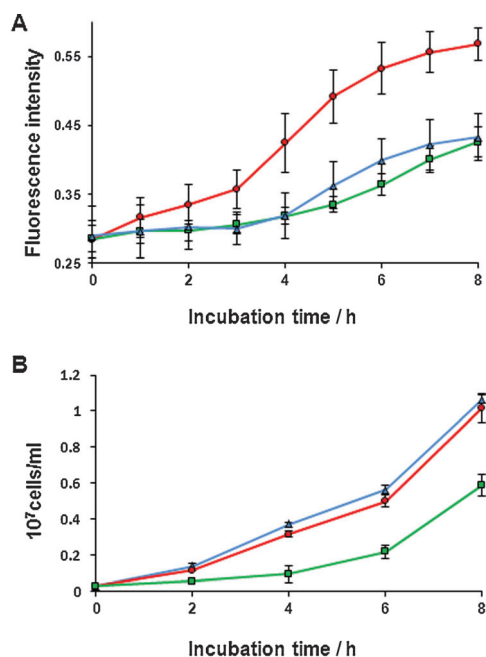The pronounced biofilm-induced color and fluorescence transformations within dip-coated sol–gel/PDA films point to

Figure 5. Sol–gel/PDA films for screening biofilm inhibitors. A) Kinetic curves of PDA fluorescence emitted from sol–gel/PDA films incubated with: (——) *P. aeruginosa*, (——) silver-doped sol–gel/PDA films incubated with *P. aeruginosa*, and (——) *P. aeruginosa* with iron chloride. B) Bacterial cell populations of *P. aeruginosa*: (——) *P. aeruginosa* with iron chloride, (——) control (no inhibitor), and (——) silver-doped sol–gel/PDA films incubated with *P. aeruginosa*.

the potential use of this platform for screening chemical substances exhibiting putative biofilm inhibitory effects. Figure 5 depicts experiments in which the silica sol–gel/PDA films were employed to probe the activity of two distinct bacterial- and biofilm-inhibitors, specifically silver colloids[30] embedded within the sol–gel matrix, and FeCl₃[31] which was added to the bacterial growth medium. The silver salt was co-dissolved in the silica/diacetylene monomer mixture. Subsequently, sol–gel encapsulated colloidal silver was prepared through in situ reduction, resulting in a random distribution of 10-50 nm colloidal silver particles throughout the silica gel matrix.

The incorporation of the silver colloids in the sol–gel/PDA framework points to the feasibility of using the silica-gel/PDA films as a "host matrix" for chemical substances that could be subsequently screened for their antibacterial or antibiofilm activities. The fluorescence kinetic graph in Figure 5 A, recorded in a multi-well microplate (excitation 544 nm, emission 620 nm) underscores the dramatic impact of the inhibitors on biofilm-induced PDA fluorescence. The control curve (—— in Figure 5 A) shows the gradually increasing fluorescence of a sol–gel/PDA film incubated in a *P. aeruginosa* suspension without inhibitors added. However, in case of both the sol–gel/PDA film suspended in a bacterial solution to which FeCl₃ had been added (—— in Figure 5 A) or the sol–gel PDA matrix that contained silver colloids (—— in Figure 5 A), a significant reduction in PDA fluorescence was observed. Similar differences in fluorescence response were apparent in fluorescence microscopy experiments (Figure 2 in the Supporting Information).

Although the fluorescence spectroscopy results in Figure 5 A clearly demonstrate the inhibitory effects of the added chemical substances on biofilm-induced PDA fluorescence, we further aimed to determine the consequences of their addition on the overall bacterial populations in the culture (Figure 5 B). Figure 5 B presents the number of bacterial cells in the culture calculated through conventional light absorption at 600 nm. Indeed, the bacterial counts depicted in Figure 5 B clearly show that the presence of film-embedded Ag colloids not only eliminated biofilm formation, but significantly reduced the number of bacterial cells in the solution (—— in Figure 5 B). In contrast, FeCl₃ did not affect the population of *P. aeruginosa* in the solution (—— in Figure 5 B), but specifically inhibited formation of the surface-deposited biofilms, likely through interference with quorum sensing pathways. Indeed, while Greenberg and co-workers have shown the importance of available iron for biofilm growth in *P. aeruginosa*,[32] Hergenrother and co-workers have reported an inhibitory effect on biofilm growth of *P. aeruginosa* for high concentrations of iron salts.[33]

Conclusion

We present an intriguing biomimetic system in which silica sol–gel/polydiacetylene thin films, prepared through a dip-coating technique, promote rapid formation of bacterial biofilms, and furthermore allows visual and microscopic investigation of both biofilm proliferation as well as biofilm inhibition. Each of the two film components has distinct roles in affecting the unique chemical and microbiological properties of the films. The sol–gel matrix stabilizes the film and constitutes a framework for embedding organized PDA domains. The conjugated PDA units have dual roles—promoting biofilm formation on the one hand, and on the other hand constitute a sensitive platform to follow biofilm deposition and identify potent biofilm inhibitors.

The spectroscopy and microscopy data demonstrate that the sol–gel/PDA thin films form a simple, easily applied, and effective platform for in situ kinetic and structural analysis of biofilm formation. The system can be also employed for analysis and for high-throughput screening of biofilm inhibitors. Indeed, the mesoporous structure of the sol–gel matrix allows incorporation of guest substances, such as the silver colloids (Figure 5), thus facilitating examination of their impact on biofilm development. Importantly, through monitoring the PDA fluorescence one can obtain specific information regarding the production of biofilm matrices, rather than bacterial proliferation in general. Accordingly, the technology allows differentiating between substances affecting bacterial growth and those that interfere with biofilm formation.

Experimental Section

Materials

The diacetylene monomer 10,12-tricosadiynoic acid was purchased from Alfa Aesar, tetraethyl orthosilicate (TEOS) at 98% purity, sodium borohydride (NaBH₄), and FeCl₃·6H₂O (97%) were pur-

chased from Sigma–Aldrich. Tetrahydrofuran (THF) and nitric acid (HNO_3) were purchased from Frutarom Ltd. Silver nitrate ($AgNO_3$) was purchased from Metalor Technologies UK Ltd. Water was doubly distilled by a Barnstead D7382 water purification system (Barnstead Thermolyne Corporation, Dubuque, IA), producing water having 18.3 MΩ cm resistivity. Glass slides were purchased from Menzel Glasser (Germany). The bacterial strains used in the experiments were *Salmonella serovar typhimurium* (strain CS093) 1a (provided by A. Porgador, Ben Gurion University) and *Pseudomonas aeruginosa* PAO1 wild-type strain.

Film preparation

The thin films were prepared through the sol–gel based dip-coating technique on glass supports, following the method described by Yang et al.[24] Briefly, solutions of precursor were synthesized from TEOS, the diacetylene monomer, and HNO_3 catalyst prepared in a THF/water solvent at room temperature. The final reactant mole ratios were 1:9:312:0.13:40 (diacetylene/TEOS/THF/HNO_3/H_2O). After one day aging at ambient temperature, the sol solution was filtered through 0.45 μm nylon and kept at $-20\,°C$ between the experiments. For deposition on glass substrates the slide was dipped in silica/PDA sol and kept immersed for 1 minute. After this, the substrate was pulled out at withdrawal speed of approximately 35 mm s^{-1}. After air-drying, uniform thin films were irradiated with ultraviolet light (254 nm) for 1 minute to produce the blue-phase polydiacetylene domains.

For silver-doped sol–gel films, silver nitrate salt was added to the dip-coating solution at a concentration of 5 mg mL^{-1}. After the coating, the prepared slides were dipped in a freshly prepared sodium borohydride/water solution (15 mg mL^{-1}) for 15 seconds each to induce silver reduction.

Bacterial growth

Bacteria were grown aerobically at $37\,°C$ in a sterilized solid Luria Bertani (LB) medium composed of 13.5% yeast extract, 27% peptone, 27% NaCl, and 32.5% agar at pH 7.4. After overnight growth, a colony from each bacterial strain was taken and added to 10 mL of sterilized LB growth medium. Bacterial concentrations in the solutions were measured by UV/Vis spectroscopy (600 nm).

Fluorescence microscopy (desktop and confocal)

Fluorescence images of the PDA domains into silica/PDA thin films were obtained on an Olympus IX70 microscope (Japan) with an UPlanFL20x/0.50 objective. Excitation was from 470 to 490 nm, and emission was at a wavelength greater than 520 nm. Prior to imaging, films were incubated in a 48-well sterile microplate with 1 mL added bacteria solution (3·10^7 cells mL^{-1}) at $37\,°C$ for different time intervals (2–8 h). After suspension, the films were washed with distilled-deionized water (DDW) and examined on the microscope.

Confocal observations of a bacteria adhered to the films were acquired using PerkinElmer UltraVIEW system (PerkinElmer Life Sciences Inc., MA, USA) equipped with Axiovert-200 M (Zeiss, Germany) microscope and an Plan-Neofluar 63×/1.4 oil objective. The excitation wavelength at 568 nm was produced by an argon/krypton laser. Emitted light was passed through a barrier filter (580–700 nm). For this assay the unpolymerized films were incubated in the multi-well sterile microplate with bacteria solution as described previously, after which the washed plate wells with the films were

filled with 0.1% crystal violet in water and gently shaken for 25 min at $37\,°C$. The stained films were washed ten times with DDW before the imaging.

Fluorescence spectroscopy

In the fluorescence kinetic experiments Thermo Scientific Fluoroskan Ascent FL (Thermo Fisher Scientific Inc., USA) was used, excitation was at 544 nm and emission was recorded at 620 nm. Samples for fluorescence kinetic measurements were prepared by adding 1 mL bacterial solutions (3·10^7 cells mL^{-1}) to the wells of 48-well microplates (Grainer Bio-one) containing polymerized (blue-phase) sol–gel/PDA films. Fluorescent chromatic responses of the films were recorded every hour during the incubation period. In order to analyze biofilm inhibition affects, *P. aeruginosa* PAO1 was grown in LB medium supplemented with 5 μL $FeCl_3$ solution (25 mM), or placed in medium upon silver-doped sol–gel/PDA films.

Scanning electron microscopy

Samples for SEM analysis were fixed in 2% glutardialdehyde and 2% paraformaldehyde buffered with 0.1 M buffer cacodilate (pH 7.2–7.4) at $4\,°C$ for 8 hours. Fixation was followed by a five-step dehydration with an ethanol/water gradient (30–100%) and by immersion in hexamethyldisilazane (HMDS)/ethanol gradient solution (30–100%) at room temperature. This process was repeated seven times. After air-drying until full evaporation of HMDS, the dehydrated specimens were further desiccated at $25\,°C$ for 24 hours and gold-coated in a sputtering device EMITECH K575x (Emitech Ltd, UK). SEM images were recorded using a Jeol JSM-7400F Scanning electron microscope (JEOL LTD, Tokyo, Japan) operated and analyzed using the instrument software.

[1] M. Habash, G. Reid, *J. Clin. Pharmacol.* **1999**, *39*, 887–898.

[2] J. W. Costerton, P. S. Stewart, E. P. Greenberg, *Science* **1999**, *284*, 1318–1322.

[3] B. Z. Fathepure, T. M. Vogel, *Appl. Environ. Microbiol.* **1991**, *57*, 3418–3422.

[4] Z. Du, H. Li, T. Gu, *Biotechnol. Adv.* **2007**, *25*, 464–482.

[5] J. W. Bartholomew, H. Finkelstein, *J. Bacteriol.* **1954**, *67*, 689–691.

[6] R. J. Palmer, C. Sternberg, *Curr. Opin. Biotechnol.* **1999**, *10*, 263–268.

[7] F. J. Louws, D. W. Fulbright, C. T. Stephens, F. J. de Bruijn, *Appl. Environ. Microbiol.* **1994**, *60*, 2286–2295.

[8] G. D. Christensen, W. A. Simpson, A. L. Bisno, E. H. Beachey, *Infect. Immun.* **1982**, *37*, 318–326.

[9] G. D. Christensen, W. A. Simpson, J. J. Younger, M. Baddour Larry, F. F. Barrett, D. M. Melton, E. H. Beachey, *J. Clin. Microbiol.* **1985**, *22*, 996–1006.

[10] R. K. Pettit, C. A. Weber, M. J. Kean, H. Hoffmann, G. R. Pettit, R. Tan, K. S. Franks, M. L. Horton, *Antimicrob. Agents Chemother.* **2005**, *49*, 2612–2617.

[11] R. W. Carpick, D. Y. Sasaki, M. S. Marcus, M. A. Eriksson, A. R. Burns, *J. Phys. Condens. Matter* **2004**, *16*, R679–R697.

[12] S. Okada, S. Peng, W. Spevak, D. Charych, *Acc. Chem. Res.* **1998**, *31*, 229–238.

[13] D. H. Charych, J. O. Nagy, W. Spevak, M. D. Bednarski, *Science* **1993**, *261*, 585–588.

[14] J. Kim, J.-M. Kim, D. J. Ahn, *Macromol. Res.* **2006**, *14*, 478–482.

[15] Z. Orynbayeva, S. Kolusheva, E. Livneh, A. Lichtenshtein, I. Nathan, R. Jelinek, *Angew. Chem.* **2005**, *117*, 1116–1120; *Angew. Chem. Int. Ed.* **2005**, *44*, 1092–1096.

[16] J. S. Kauffman, B. M. Ellerbrock, K. A. Stevens, P. J. Brown, W. T. Pennington, T. W. Hanks, *ACS Appl. Mater. Interfaces* **2009**, *1*, 1287–1291.

[17] S. Kolusheva, L. Boyer, R. Jelinek, *Nat. Biotechnol.* **2000**, *18*, 225–227.

[18] C. K. Park, C. D. Kang, S. J. Sim, *Biotechnol. J.* **2008**, *3*, 687–693.

[19] D. Meir, L. Silbert, R. Volinsky, S. Kolusheva, I. Weiser, R. Jelinek, *J. Appl. Microbiol.* **2008**, *104*, 787–795.

[20] L. Silbert, I. Ben Shlush, E. Israel, A. Porgador, S. Kolusheva, R. Jelinek, *Appl. Environ. Microbiol.* **2006**, *72*, 7339–7344.

[21] J.-M. Kim, Y. B. Lee, S. K. Chae, D. J. Ahn, *Adv. Funct. Mater.* **2006**, *16*, 2103–2109.

[22] D. J. Ahn, J.-M. Kim, *Acc. Chem. Res.* **2008**, *41*, 805–816.

[23] Y. Demikhovsky, S. Kolusheva, M. Geyzer, R. Jelinek, *J. Colloid Interface Sci.* **2011**, *364*, 428–434.

[24] Y. Yang, Y. Lu, M. Lu, J. Huang, R. Haddad, G. Xomeritakis, N. Liu, A. P. Malanoski, D. Sturmayr, H. Fan, D. Y. Sasaki, R. A. Assink, J. A. Shelnutt, F. van Swol, G. P. Lopez, A. R. Burns, C. J. Brinker, *J. Am. Chem. Soc.* **2003**, *125*, 1269–1277.

[25] C. J. Brinker, G. C. Frye, A. J. Hurd, C. S. Ashley, *Thin Solid Films* **1991**, *201*, 97–108.

[26] F. Gaboriaud, R. Golan, R. Volinsky, A. Berman, R. Jelinek, *Langmuir* **2001**, *17*, 3651–3657.

[27] R. W. Carpick, D. Y. Sasaki, A. R. Burns, *Langmuir* **2000**, *16*, 1270–1278.

[28] T. R. De Kievit, R. Gillis, S. Marx, C. Brown, B. H. Iglewski, *Appl. Environ. Microbiol.* **2001**, *67*, 1865–1873.

[29] M. E. Buck, A. S. Breitbach, S. K. Belgrade, H. E. Blackwell, D. M. Lynn, *Biomacromolecules* **2009**, *10*, 1564–1574.

[30] N. Stobie, B. Duffy, D. E. McCormack, J. Colreavy, M. Hidalgo, P. McHale, S. J. Hinder, *Biomaterials* **2008**, *29*, 963–969.

[31] L. Yang, K. B. Barken, M. E. Skindersoe, A. B. Christensen, M. Givskov, T. Tolker-Nielsen, *Microbiology* **2007**, *153*, 1318–1328.

[32] P. K. Singh, M. R. Parsek, E. P. Greenberg, M. J. Welsh, *Nature* **2002**, *417*, 552–555.

[33] D. J. Musk, D. A. Banko, P. J. Hergenrother, *Chem. Biol.* **2005**, *12*, 789–796.